Available online at www.sciencedirect.com
SCIENCE DIRECT®
Nuclear Instruments and Methods in Physics Research A 505 (2003) 568–572
NUCLEAR INSTRUMENTS & METHODS IN PHYSICS RESEARCH Section A
www.elsevier.com/locate/nima

Evaluation of a computer aided neutron tomographic system incorporating a gaseous position sensitive detector

M.I. Silvani[a], R.T. Lopes[b,*], E.F.O. de Jesus[b], G.L. de Almeida[a], A.F. Barbosa[c]

[a] *Instituto de Engenharia Nuclear - CNEN, Caixa Postal 68550, Rio de Janeiro 21945-970, Brazil*
[b] *Nuclear Instrumentation Laboratory, COPPE-Universidade Federal do Rio de Janeiro, Caixa Postal 68509, Rio de Janeiro 21945-970, Brazil*
[c] *Centro Brasileiro de Pesquisas Físicas—CNPq, R. Dr. Xavier Sigaud, 22290-180 Rio de Janeiro, Brazil*

Abstract

A position sensitive gaseous detector, formerly designed to operate with X-rays, has been modified to equip a third generation tomographic system working with a parallel thermal neutron beam. For this purpose, the original filling-gas has been replaced by ^{3}He-enriched helium, which plays simultaneously the role of filling-gas for the ionization process and converter of neutrons into charged particles. This paper describes the modifications done to the detector, the measurements carried out to evaluate its own performance and that of the tomographic system attached to it. Some tomographic images acquired using that system are presented as well. Tomographic systems equipped with this kind of detector should require substantially much less time than those conventional ones, where a sample translation is required. The *Argonauta* reactor operating at the *Instituto de Engenharia Nuclear (IEN/CNEN-Brazil)* has been utilized as the source of neutrons, furnishing a flux of $4.5 \times 10^5\,\mathrm{n\,cm^{-2}\,s^{-1}}$ at its main irradiation channel where the tomographic system has been placed.

PACS: 87.59.F; 28.20.F; 29.40.C

Keywords: Computed tomography; Thermal neutrons; Position sensitive detector

1. Introduction

The gaseous Position Sensitive Detector—PSD, described in this work operates at the proportional region and is constituted by a gas chamber containing a multi-strip flat cathode. A wire placed between this cathode and the detector window acts as anode like in the conventional detectors.

The electron avalanche produced near the anode induces a charge distribution in the cathode strips, which are connected to a delay line as shown in Fig. 1. The electronic signal produced by that charge distribution propagates in both directions toward the extremities of that line. A comparison of the time lapses required by both signals to arrive at the end of each line allows the determination of the traveled distances, defining thus the position where the ionizing event occurred [1].

To detect neutrons, the detector should contain a material with a high absorption cross-section,

*Corresponding author. Tel.: +55-21-2562-7308; fax: +55-21-2562-8444.
E-mail address: ricardo@lin.ufrj.br (R.T. Lopes).

0168-9002/03/$ - see front matter
doi:10.1016/S0168-9002(03)01149-5

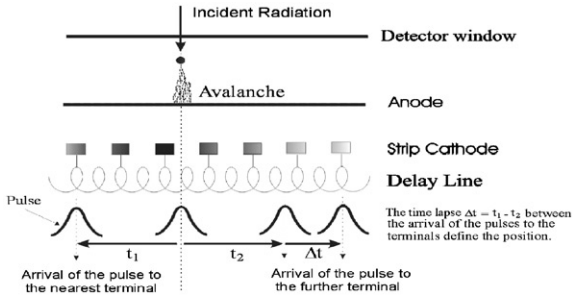

Fig. 1. Operation principle of a *Position Sensitive Detector*.

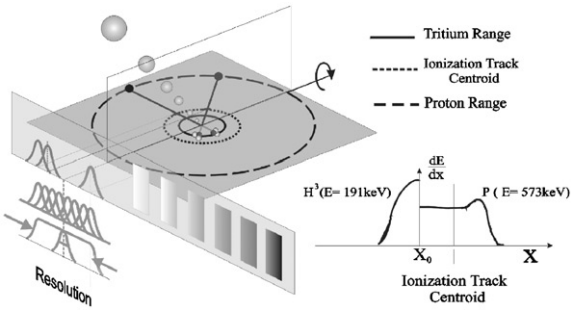

Fig. 2. Scheme illustrating the shift of the neutron position as *seen* by the detector with regard to its actual incidence position.

capable to produce an ionizing radiation after its interaction with those particles. The most commonly used materials to convert neutrons into charged particles, are ^{10}B, ^{6}Li, ^{3}He and natural gadolinium [2,3]. In this work ^{3}He-enriched helium under a 3 atm pressure, has been utilized as filling gas, acting as neutron-to-charged particle converter and ionization medium. The carbon window mounted into a stainless steel frame formerly used in the original X-ray detector, has been replaced by a single piece cast in aluminum.

The proton and tritium products of the $^{3}He(n,p)^{3}H$ nuclear reaction are isotropically emitted into opposite directions carrying 573 and 191 keV, respectively. Each particle generates its own ionization track which centroid is shifted from the point where the reaction occurred, due to the different particle ranges. This shift degrades the detector spatial resolution as explained below [4].

All ionization tracks centroids around a point where the nuclear reaction occurs are distributed over a spherical layer. Disregarding the beam hardening, i.e., assuming a thin layer, the probability density for the centroids distributed along a parallel line to the anode wire is a rectangular function with a width limited by the external diameter of that spherical layer. The position where a nuclear reaction occurs inside the detector is ultimately computed from the charge distribution induced on its cathode, and the centroid of this distribution is defined by the projection of the weigh center of all centroids on the cathode axis. Therefore, when a narrow thermal neutron beam hits the detector window on a perpendicular direction the expected peak becomes flattened due to the above-mentioned phenomena, and hence the spatial resolution is degraded. Fig. 2 shows a scheme of this process.

2. Detector performance

The detector performance is characterized by quantitative parameters such as spatial resolution, linearity and homogeneity [5]. These parameters as well as the detector response are shown in Fig. 3.

In Fig. 3c, the maximal channel deviation with regard to the fitted straight line is less than 0.7% over the entire detector active length. For a monoenergetic source, the *homogeneity* of a PSD is defined as the maximal deviation from the average counts obtained at all cells. The correspondent detector homogeneity for an average of 12,000 counts/channel is shown in Fig. 3d.

3. Tomographic images

The assembled tomographic system is schematized in Fig. 4. The *Argonauta* reactor at *Instituto de Engenharia Nuclear (IEN/CNEN-Brazil)* has been utilized as the source of thermal neutrons, furnishing a flux of $4.5 \times 10^{5}\,n\,cm^{-2}\,s^{-1}$.

To obtain a figure of merit for the tomographic systems equipped with the PSD, two characteristics have been evaluated: the *Modulation Transfer Function-MTF* and the *Resolution Distance* [6]. From the MTF curve, it's possible to infer

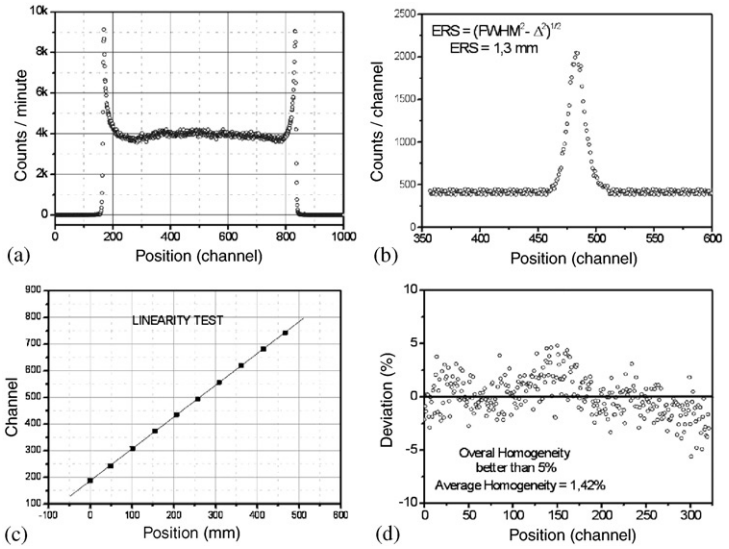

Fig. 3. (a) Response of the PSD detector. (b) Resolution determined using a simulated line source. (c) Linearity between a channel in the spectrum for a given slit and its actual position on the detector window. (d) Detector homogeneity for 12 k counts.

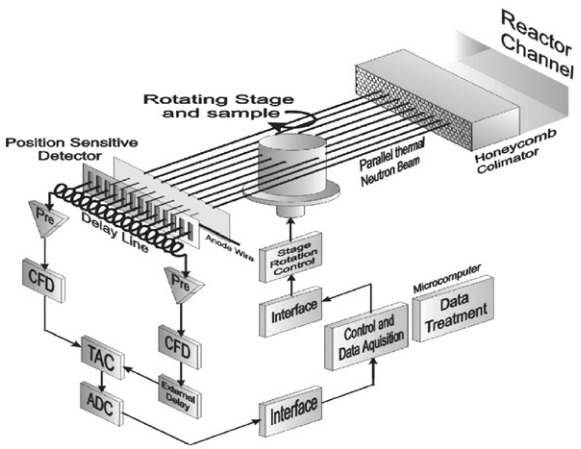

Fig. 4. Computed neutron tomographic system with a gaseous PSD.

approximately the minimal size of a feature recognized by the system as a single entity, while the Resolution Distance furnishes the minimal distance between two features capable to be individually recognized by the system as that.

The MTF curve, including the cutoff at 10%, is shown in Fig. 5a. It is generally accepted that below that value a tomographic system is unable to reproduce an image with an acceptable quality.

The determination of the Resolution Distance has been carried out by replacing the object to be tomographed by gadolinium masks containing one pair of slits. These slits had always the same 1 mm-aperture, but were separated by a variable distance within the range 1.2–4.8 mm. The points of the Resolution Distance curve correspond to the percent ratio of the difference between the counts at the peak and the counts at the valley, to the counts at the peak, after a background subtraction. A polynomial curve has been fitted to these points for the sake of an easier interpolation. The cutoff value at 10% corresponds to a Resolution Distance of 1.31 mm between the slits.

The test-bodies used to get the tomographic images were constituted by 23 mm-diameter aluminum and Teflon cylindrical rods provided with 3 mm-diameter orifices, filled with materials usually applied in the engineering field.

Tomographic images of different arrangements have then be obtained to evaluate some potential uses for the thermal neutron radiography. Images of metallic and plastic materials in a Teflon matrix are shown in Figs. 6a and b, respectively. Besides the high contrast produced by those hydrogen-bearing materials a visual inspection of these images obtained under similar conditions allows

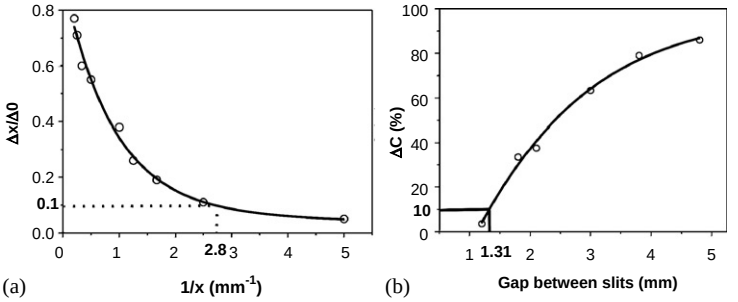

Fig. 5. (a) MTF curve for the Tomographic System. Δx and $\Delta 0$ are the intensities of the transmitted and incident beam, respectively. (b) Resolution Distance curve. $\Delta C = 10\%$ for slits 1.31 mm apart.

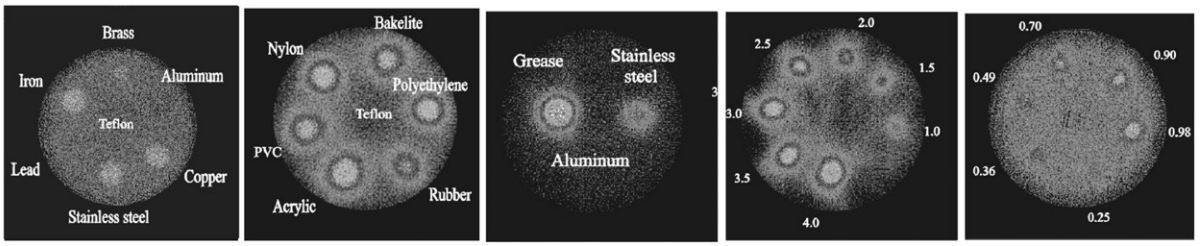

Fig. 6. Tomographic images obtained with thermal neutrons and a gaseous PSD. Samples (a)–(c) are constituted by a 23 mm-diameter aluminum or teflon cylinder provided with 3 mm-diameter orifices filled with different materials. Samples (d) and (e) contain gadolinium oxide and cadmium, respectively, in a teflon matrix, where the labels refer to the orifice diameters.

an ordering according to their color tonality as follows:

$$Al < \text{rubber} < PVC \approx \text{bakelite} < \text{lucite} < \text{nylon} \approx C_2H_4$$

which is consistent with the respective macroscopic cross-section: $0.09 < 0.97 < 2.48 \approx 2.50 < 2.62 < 3.16 \approx 3.49$

From Fig. 6c it is easy to realize that grease is a better neutron absorber than aluminum and stainless steel, making feasible the detection of its presence in lubrication channels, for instance.

To verify the influence of the *spatial resolution* on the image of a real object rather than a slit, tomographies of two 23 mm-diameter teflon cylindrical rods, provided with orifices of different diameters have been carried out. One of the rods contained 7 orifices with diameters varying within the range 1–4 mm, filled up with gadolinium oxide. The other rod contained six 0.28–0.98 mm-diameter orifices, filled up with cadmium wires.

The obtained images are shown in Figs. 6d and e, where it can be observed that system detects the presence of gadolinium and cadmium in *all* the orifices, although only until 0.36 mm if a reasonable resolution is required, as foreseen by the MTF curve.

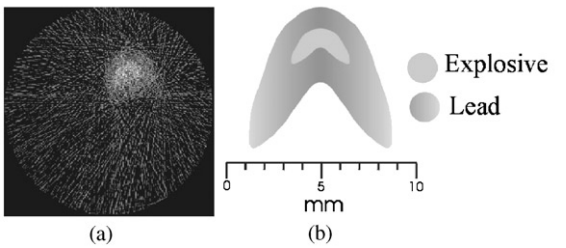

Fig. 7. (a) Tomography of a lead gasket containing an explosive stuff kernel. (b) Scheme of the tomographed gasket slice.

This neutron tomographic system, could be potentially used by industries of explosives, as suggested by Fig. 7, which displays the cross-section image of a lead explosive gasket used in the air-space industry. Plastic explosives as well,

contains hydrogen and are usually surrounded by heavy materials such as lead or steel, making their detection difficult by X-rays but feasible by neutrons.

When an inspection utilizing neutrons is performed, they travel practically free in metallic hulls like lead or steel but are strongly attenuated by hydrogen-bearing explosives, producing thus a good contrast. Hence, besides a control of the correct positioning of the explosive itself inside its hull, voids, density variations or the presence alien materials can be detected.

4. Conclusion

The developed thermal neutron PSD, not only detects the presence of neutron-attenuating materials, where X-rays detection would not work properly, but also does it very well even for small-sized objects. Although a first generation system could yield a similar or even better resolution by narrowing the collimator aperture [7], the acquiring time should correspondingly be lengthened in order to keep an acceptable statistics assuring, thus a good image quality, and to deal with the required additional table translation movement. The scope of this work limited the detector modifications to the replacing of the original argon–methane filling-gas by ^{3}He-enriched helium. In spite of it, the promising obtained results have shown that further efforts should be done towards the development of a specific neutron-fashioned PSD, improving thus its resolution and efficiency, which would emerge as better image quality and lessened acquiring times for a tomographic system equipped with it.

References

[1] A. Gabriel, Rev. Sci. Instrum. 10 (1980) 1303.
[2] J. Alberi, J. Fischer, V. Radeka, L.C. Rogers, B. Schoenborn, Nucl. Instr. and Meth. 127 (1975) 507.
[3] A.P. Jeavons, N.L. Ford, B. Lindeberg, R. Sachot, IEEE Trans. Nucl. Sci. NS-25 (1) (1978) 553.
[4] R.A. Boie, J. Fisher, Y. Inagaki, F.C. Merritt, H. Okuno, V. Radeka, Nucl. Instr. and Meth. 200 (1982) 533.
[5] A.F. Barbosa. Report CBPF-CNPq Brazil NF-068/94, 1994.
[6] ASTM E 1441-95 and 1570-95a, Guide for Imaging and Practice for Examination, ISSO/TC 135/SC 5, N 118, 1996.
[7] G.L. de Almeida, M.I. Silvani, R.T. Lopes, International Nuclear Atlantic Conference INAC, Rio de Janeiro, Brazil, August, 2002.